



**HAL**  
open science

## Association of partially-folded lens betaB2-crystallins with the alpha-crystallin molecular chaperone

Paul Evans, Christine Slingsby, B A Wallace

► **To cite this version:**

Paul Evans, Christine Slingsby, B A Wallace. Association of partially-folded lens betaB2-crystallins with the alpha-crystallin molecular chaperone. *Biochemical Journal*, 2007, 409 (3), pp.619-699. 10.1042/BJ20070993 . hal-00478853

**HAL Id: hal-00478853**

**<https://hal.science/hal-00478853>**

Submitted on 30 Apr 2010

**HAL** is a multi-disciplinary open access archive for the deposit and dissemination of scientific research documents, whether they are published or not. The documents may come from teaching and research institutions in France or abroad, or from public or private research centers.

L'archive ouverte pluridisciplinaire **HAL**, est destinée au dépôt et à la diffusion de documents scientifiques de niveau recherche, publiés ou non, émanant des établissements d'enseignement et de recherche français ou étrangers, des laboratoires publics ou privés.

**Association of Partially-Folded Lens  $\beta$ B2-Crystallins with the  $\alpha$ -Crystallin**

**Molecular Chaperone**

Paul Evans, Christine Slingsby and B.A. Wallace

Department of Crystallography, Birkbeck College, and the Institute of Structural Molecular  
Biology, University of London, London, WC1E 7HX, United Kingdom

Address correspondence to: Christine Slingsby, Department of Crystallography, Birkbeck  
College, Malet Street, London, WC1E 7HX. Tel. 44-207-631-6832; Fax. 44-207-631-  
6803; E-Mail: c.slingsby@mail.cryst.bbk.ac.uk

Short Title: Chaperone-Associated Unfolding of  $\beta$ B2-Crystallin

Keywords: Chaperone, aggregation, stability, unfolding, crystallin, cataract

Abbreviations: CD, Circular Dichroism; CSA, Camphor Sulphonic Acid

Word count text +refs+legends = 6275

### Summary

Age-related cataract is a result of crystallins, the predominant lens proteins, forming light scattering aggregates. In the low protein turnover environment of the eye lens, the crystallins are susceptible to modifications that can reduce stability, increasing the probability of unfolding and aggregation events occurring. It is hypothesised that the  $\alpha$ -crystallin molecular chaperone system recognises and binds these proteins before they can form the light scattering centres that result in cataract, thus maintaining the long-term transparency of the lens. In this study we investigated the unfolding and aggregation of (wildtype) human and calf  $\beta$ B2-crystallins, and the formation of a complex between  $\alpha$ -crystallin and  $\beta$ B2-crystallins under destabilising conditions. Human and calf  $\beta$ B2-crystallin unfold through a structurally similar pathway, but the increased stability of the C-terminal domain of human  $\beta$ B2-crystallin relative to calf  $\beta$ B2-crystallin results in the increased population of a partially folded intermediate during unfolding. This intermediate is aggregation prone, and prevents constructive refolding of human  $\beta$ B2-crystallin, whilst calf  $\beta$ B2-crystallin can refold with high efficiency.  $\alpha$ -crystallin can effectively chaperone both human and calf  $\beta$ B2-crystallin from thermal aggregation, though chaperone-bound  $\beta$ B2-crystallins are unable to refold once returned to native conditions. Ordered secondary structure is seen to increase in  $\alpha$ -crystallin with elevated temperatures up to 60° C; structure is rapidly lost at temperatures of 70° C and above. Our experimental data combined with previously reported observations of  $\alpha$ -crystallin quaternary structure have lead us to propose a structural model of how activated  $\alpha$ -crystallin chaperones unfolded  $\beta$ B2-crystallin.

## **Introduction**

The transparency and refractive power of the vertebrate eye lens is achieved by the high concentration and regular spatial distribution of crystallin proteins [1,2]. In the low protein turnover environment of the lens, transparency is maintained by the intrinsic stability, solubility, and longevity of these crystallins; disturbances in lens transparency inevitably result in cataract [3].

The three classes of crystallins,  $\alpha$ ,  $\beta$  and  $\gamma$  are members of two large gene families: the  $\alpha$ -crystallins, which are members of the widely distributed small heat shock protein family, function both as molecular chaperones and structural proteins [4] and the more lens specific structural  $\beta\gamma$ -crystallins [5]. Lens optical quality and refractive power stems from a gradient of protein concentration along the optical axis, formed from differing proportions of these crystallin classes. Relative amounts of crystallin present in young human lenses are approximately 28% ( $\alpha$ ), 43% ( $\beta$ ), and 28% ( $\gamma$ ) [6,7,8]. The core of the lens is enriched in  $\gamma$ -crystallins, with the predominantly expressed being  $\gamma$ C,  $\gamma$ D, and  $\gamma$ S in humans [6,8]. Mammalian  $\beta$ -crystallins can be divided into acidic ( $\beta$ A1,  $\beta$ A2,  $\beta$ A3,  $\beta$ A4) and basic ( $\beta$ B1,  $\beta$ B2,  $\beta$ B3) forms;  $\beta$ B2 is the predominant  $\beta$ -crystallin in the human lens, contributing 14-20% of total lens protein [7,8]. Lens  $\alpha$ -crystallin is formed from two polypeptide chains,  $\alpha$ A-, and  $\alpha$ B-crystallin, which have sequence identity of approximately 56%; ratios of  $\alpha$ A- to  $\alpha$ B-crystallin in the human lens vary with age. Both  $\alpha$  and  $\beta\gamma$ -crystallins undergo extensive post-translational modifications, with deamidation appearing to correlate with loss of solubility [9].

$\alpha$ -crystallins are present in the lens as polydisperse hetero-oligomers of  $\alpha$ A- and  $\alpha$ B-crystallin. Tardieu and co-workers reported that native calf lens  $\alpha$ -crystallin assemblies consist of 40-45 subunits, with an external dimension of 170 Å [10,11], whilst others have reported a range of assembly sizes [12]. This diversity, as well as diversity arising from post-translational modifications, has thus far prevented crystallisation. Homologous small heat shock proteins from archaea, wheat, and tapeworm, have revealed the structure of the conserved  $\alpha$ -crystallin domain but in each instance variation in modes of association result in substantial differences in oligomeric assembly [13,14,15]. The chaperone function for plant small heat shock proteins is thought to be driven by the temperature-regulated increase in oligomer dissociation resulting in the population of a sub-assembly species (possibly a dimer) that provides the binding sites for non-native substrates [14,16,17]. Similarly, dissociation of mammalian HSP27 oligomers to smaller multimeric species is correlated with binding competency: the interaction between HSP27 and destabilised T4 Lysozyme has been used to propose a model in which the folding equilibrium of T4 is coupled to the oligomeric equilibrium of HSP27 [18]. This coupling offers a novel explanation for certain congenital cataracts, allowing gain of function mutations in  $\alpha$ A-crystallin to promote unfolding of substrate proteins [19]. The active form of  $\alpha$ -crystallin remains undetermined. Lens  $\alpha$ -crystallin subunit exchange is extremely rapid, and has been shown to increase with elevated temperature [20,11]. It has been proposed that transient dissociation of the oligomeric form to yield free subunits, as a result of

phosphorylation or an increase in temperature, is associated with the activation of binding or chaperone activity [21,22]. Contrastingly, in yeast small heat shock protein Hsp26 dissociation of the oligomer is not required for chaperone activity [23]. It has been suggested that the structural changes of  $\alpha$ -crystallin in response to increased temperature support a possible “activation” step in the chaperone mechanism [11].

Monomeric  $\gamma$ -crystallins and oligomeric  $\beta$ -crystallins both consist of two domains, with each domain composed of two intercalated Greek key motifs [24]. These domains pair intra-molecularly in  $\gamma$ -crystallins, via a V-shaped linker peptide, whilst in the case of  $\beta$ B2-crystallins the linker is extended and domains pair inter-molecularly, promoting oligomeric assembly [25]. However, in truncated  $\beta$ B1-crystallin the domains pair intramolecularly, like  $\gamma$ -crystallins, with this oligomer using a new interface for assembly [26, 27]. Like the  $\alpha$ -crystallins, the oligomeric  $\beta$ -crystallins engage in subunit-exchange, creating diversity [28].

Long-term stability is essential for crystallins to remain folded, thus minimising aggregation [3].  $\beta$ B1-crystallin and especially  $\gamma$ -crystallins, typically exhibit high thermodynamic stability and, sometimes, kinetic stabilisation to prevent protein unfolding [29,30,31]. However, ageing crystallins are susceptible to modification that can lower stability and/or solubility and increase the likelihood of aggregation, leading to cataract as the binding capacity of  $\alpha$ -crystallin is exceeded [32,33]. Recent studies have sought to address the structural mechanisms of  $\beta\gamma$ -crystallin unfolding and aggregation, and  $\alpha$ -crystallin chaperone activity. In the case of human  $\gamma$ D-crystallin, it has been shown to unfold by a three state mechanism at pH 7 in which the N-terminal domain unfolds first, followed by the C-terminal domain. During refolding, when the C-terminal domain folds first and acts as a nucleating centre for folding of the N-terminal domain, an aggregation-prone intermediate occurs [30,34,35]. Similarly, dimeric rat  $\beta$ B2-crystallin at low concentrations unfolds by a three-state model, in which the N-terminal domain unfolds and the dimer dissociates, resulting in a monomeric partially folded intermediate that unfolds in a second transition; at higher protein concentrations, the unfolding appears to be two-state [36]. In the presence of chemical denaturants  $\alpha$ -crystallins have lower conformational stability than  $\gamma$ - and  $\beta$ B1-crystallin [5], but broadly similar to  $\beta$ B2-crystallin and acidic  $\beta$ -crystallins [28]. Mchaourab and co-workers have studied the association between destabilised mouse  $\beta$ B2 mutants and  $\alpha$ A/ $\alpha$ B-crystallin, and have suggested that population of a folding intermediate, rather than a specific energy threshold alone, can trigger chaperone activity [37].

In this study we have examined the stability of partially folded intermediate states of  $\beta$ B2-crystallins. Two orthologues of  $\beta$ B2-crystallin, human and calf, have been studied because of differences in their thermal aggregation properties; calf  $\beta$ B2 unfolds reversibly with the unfolded form remaining soluble at high temperatures [38], whilst human  $\beta$ B2 becomes less soluble on unfolding [28]. These proteins have 97 % sequence identity, differing by one residue in the N- and C-terminal extensions, and four residues in the C-terminal domain (Fig. 1a, b). This study examines how these crystallins

differentially unfold and aggregate, and the structural changes that occur when they interact with calf lens  $\alpha$ -crystallin following thermal challenge.

## **Experimental**

### *Materials*

Recombinant human  $\beta$ B2-crystallin [27] and calf lens  $\beta$ B2- and calf lens  $\alpha$ -crystallins [39] were supplied by Dr. O. Bateman, Birkbeck College. Calf lens  $\alpha$ -crystallin was purified, as described in reference 39, by gel filtration on Sephacryl S-300HR, taking care to exclude the high molecular weight shoulder (HMW) of alpha-crystallin. Bovine  $\alpha$ -crystallin has been shown to consist of  $\alpha$ A- and  $\alpha$ B-crystallin at an approximate ratio of 3:1 [4]. Samples were buffer-exchanged into 10 mM sodium phosphate buffer (pH 7.0), using Amicon Microcon10 micro-concentrator vessels, and frozen into individual aliquots.

### *Fluorometry and light scattering*

Fluorescence emission spectra were collected using a thermostatically controlled Hitachi F-2500 spectrometer, calibrated using a rhodamine B standard. Tryptophan residues were excited at 280 nm. Emission spectra were collected from 300 to 450 nm at a scan speed of 600 nm/minute. Excitation and emission slit widths were set to 10 nm, except where stated differently in the text.

Light scattering was measured with excitation and emission wavelengths set to 360 nm, and slit widths set to 10 nm, unless otherwise noted. Samples were at 0.2 mg ml<sup>-1</sup> concentration, in a 1 cm pathlength quartz cuvette (Hellma, Germany). Baseline data of buffer alone were collected under identical parameters and subtracted. Samples for fluorescence and light scattering experiments were in 10 mM sodium phosphate buffer (pH 7.0).

### *Circular Dichroism (CD) Measurements and Analyses*

CD spectra were collected at 0.2 nm steps from 280 nm to 178 nm, using an Aviv 62DS (Aviv Biomedical, USA) instrument calibrated using 99% pure camphor-10-sulphonic acid (CSA) (Sigma Aldrich) [40]. Three scans of each sample and the equivalent baseline were collected. Sample spectra were averaged across the three repeats, and averaged baselines of buffer (10 mM sodium phosphate buffer, pH 7.0) or urea subtracted. Sample concentrations were 0.2 mg ml<sup>-1</sup>, determined by absorbance at 280 nm, and the cell pathlength was 0.5 mm.

Protein secondary structures were calculated using the Contin-LL algorithm [41] and the Org48\* reference dataset [42] (Org48 with a single inaccurate spectrum removed [43]).

### *Aggregation Assays*

The amount of protein lost from a solution of  $\beta$ B2-crystallin by aggregation was measured by heating 0.2 mg ml<sup>-1</sup> aliquots in 10 mM sodium phosphate buffer (pH 7.0) to increasing temperatures for ten minutes,

removing the heated sample and cooling on ice for five minutes, centrifuging for five minutes in a bench-top microfuge. The UV-absorbance at 280 nm of the supernatant was measured before heating, and after incubation at each temperature.

#### *Unfolding Assays*

Thermal denaturation experiments were performed as follows: Samples at a protein concentration of 0.2 mg ml<sup>-1</sup>, in 10 mM Na phosphate, pH 7.0, were incubated for 10 minutes at a given temperature before CD measurements were obtained at a single wavelength (195 nm). Refolded samples were first unfolded at the elevated temperature for 10 minutes then refolded for 15 minutes at 20° C. In each experiment fresh samples were used for each temperature step.

Chemical denaturation was performed as follows: stock solutions of 7 M urea ( $\geq 99.5\%$  purity, Sigma Aldrich) were prepared in 10 mM sodium phosphate buffer (pH 7.0) and the exact urea concentration determined by measuring the refractive index using an ABBE mark II refractometer (Reichert, USA).  $\beta$ B2-crystallin samples were incubated at 20° C for 16 hours in urea solutions of increasing concentration, at 0.2 mg ml<sup>-1</sup>. Samples were centrifuged for five minutes in a bench-top microfuge prior to data collection. CD measurements were obtained at a single wavelength (222 nm, because the absorbance of the urea prevented measurements being obtained at 195 nm).

#### *Preparation of the Crystallin and Chaperone Complexes*

Samples of  $\alpha$ -crystallin and  $\beta$ B2-crystallin were incubated together at 4° C, with each component at a concentration of 0.2 mg ml<sup>-1</sup> (equivalent to molar concentrations of 10.1  $\mu$ M and 8.6  $\mu$ M for  $\alpha$ -crystallin and  $\beta$ B2-crystallin, respectively, based on the molecular weight of individual polypeptide chains; a 1:1.17 excess of  $\alpha$ -crystallin), for 48 hours prior to experiments. The buffer for these experiments was 10 mM sodium phosphate (pH 7.0). Solutions of  $\alpha$ -crystallin and  $\beta$ B2-crystallin were incubated at 60° C in a circulating water bath, with separate control samples of  $\alpha$ -crystallin, and human and bovine  $\beta$ B2-crystallins. Samples were removed from incubation after 16 hours, cooled on ice for five minutes, centrifuged for five minutes in a bench-top microfuge, loaded into demountable quartz cuvettes of appropriate pathlength (Hellma, Germany), and equilibrated for ten minutes at 20 °C in the CD instrument prior to data collection.

## Results

### *Unfolding and refolding of $\beta$ B2-Crystallin*

The studies of Bateman and co-workers indicated that calf and human  $\beta$ B2-crystallin exhibit different solubilities at elevated temperature, with human  $\beta$ B2 becoming insoluble at higher temperatures [28]. The aggregation of human and calf  $\beta$ B2 was investigated to identify the structure/stability basis for these observations.

Aliquots of  $\beta$ B2-crystallin were incubated at increasing temperature, cooled and centrifuged to remove aggregated material, then UV absorbance measured to monitor changes in concentration due to heating. Calf  $\beta$ B2 remains soluble following incubation at temperatures up to 90° C, whilst human  $\beta$ B2-crystallin aggregates extensively above 50° C (Fig. 2a). Non-centrifuged samples of human  $\beta$ B2 exhibit intense light scattering above 50° C, whilst scattering from calf  $\beta$ B2 is minimal (Fig. 2b). These observations confirm those of Bateman and co-workers, and reflect substantially different behaviour between the two  $\beta$ B2 orthologues.

$\beta$ B2 unfolding during thermal and chemical denaturation was measured using circular dichroism. Calf  $\beta$ B2-crystallin unfolds in an apparent two-state process with a  $T_m$  of approximately 62° C, as indicated by the sigmoid unfolding curve of Fig. 3a and isodichroic point in Fig. 4a. Urea-induced unfolding occurs with a  $C_{1/2, \text{urea}}$  of approximately 1.6 M (Fig. 3b). Conversely, human  $\beta$ B2 unfolds through two distinct transitions as monitored by the onset of light scattering and aggregation (Fig. 3a).  $T_m$  values for the two transitions are 64° C and 78° C, respectively, and the mid-point of the inter-phase plateau is 74° C (Fig. 3a). Urea denaturation confirms the biphasic unfolding of human  $\beta$ B2, with approximated  $C_{1/2, \text{urea}}$  values for the transitions of 2.2 M and 3.4 M, respectively (Fig. 3b). Both thermal and chemical denaturation curves show the intermediate as ~33% folded. As the relative stability of human  $\beta$ B2 exceeds that of calf, it appears that the less stable protein is in fact more soluble at higher temperature, from which it can be inferred that the unfolded state exhibits greater solubility than the partially folded state.

Refolding of  $\beta$ B2-crystallins was assessed by recording CD spectra of proteins at elevated temperatures, then refolding from each of these temperature steps at 20° C. Spectra of refolded calf  $\beta$ B2 samples are similar to those of unheated  $\beta$ B2 at 20° C, confirming a return to the folded state (Fig. 4b). Differences in CD magnitude are due to a small loss of material during the heating, cooling and data collection process, indicating that an aggregation-prone earlier pathway exists alongside the productive refolding pathway. During unfolding, CD spectra of human  $\beta$ B2 are very similar to their fully folded and fully unfolded calf counterpart; however, an isodichroic point is not observed during human  $\beta$ B2 unfolding (Fig. 4c). Above 60° C, human  $\beta$ B2 does not fully refold to the native structure, appearing partially folded (Fig. 4d). Refolded spectra show increased absorbance due to light scattering, indicating



that the spectra may include contributions from insoluble aggregate material as well as soluble protein. Previous biophysical characterisation of human  $\beta$ B2-crystallin has shown no change in molecular weight upon refolding from denaturing concentrations of urea [27].

At concentrations used in this study, calf  $\beta$ B2 unfolds in a two-state manner ( $N_2 \leftrightarrow 2U$ ) similar to that proposed for higher concentrations of rat  $\beta$ B2-crystallin [36]; this cannot rule out a scarcely populated monomeric intermediate state. Human  $\beta$ B2 unfolds according to the three state model proposed by Liang and co-workers [44], but as unfolding is not fully reversible the unfolding process is better described as ( $N_2 \rightarrow 2I \rightarrow 2U$ ). In this work the human  $\beta$ B2 intermediate appears ~33% folded, as defined by the magnitude of the CD signal at 195 and 222 nm, in agreement with published fluorometry data [44,45], suggesting that the intermediate (monomeric with unfolded N-terminal domain) may also exhibit loss of structure within the predominantly folded C-terminal domain. Population of this intermediate marks the divergence of an aggregation-prone pathway, similar to the proposed mechanism for the aggregation of human  $\gamma$ D-crystallin during refolding [34].

As studies of rat  $\beta$ B2 mutants showed that removal of the extensions does not alter the stability or unfolding profiles of the protein [46], it is unlikely that sequence differences in these could contribute to the increased stability of human  $\beta$ B2. Comparison of human [27] and bovine (2BB2 [25])  $\beta$ B2-crystallin structures reveal no differences in hydrogen bonding at sites of sequence variation other than one additional hydrogen bond between Asp<sup>172</sup> and Ser<sup>174</sup> of human  $\beta$ B2. The increased stability of human  $\beta$ B2 may therefore be due to stabilisation of the loop between strands C4 and D4.

CD and tryptophan fluorometry were used to study aggregated material, before and after centrifugation, obtained from unfolded samples of human  $\beta$ B2. The spectrum of the aggregate, determined as the difference between samples before and after centrifugation, is consistent with the aggregate having a high content of  $\beta$ -sheet, and appears more structured than the soluble, partially refolded,  $\beta$ B2 (Fig. 5). Fluorometry  $\lambda_{\max}$  emission measurements were collected from native (328 nm), unfolded (347 nm) and refolded (338 nm pre/post-centrifugation) human  $\beta$ B2 samples, suggesting partial burying of tryptophan residues in both the refolded and aggregated states (data not shown). The failure of the soluble material to fully refold may indicate that it is trapped in a low energy, non-native state.

#### *Stability and secondary structure of $\alpha$ -crystallin*

Chaperone assays frequently rely on temperature to promote substrate protein aggregation [4,47] and to activate  $\alpha$ -crystallin [11]. Accordingly, identifying the maximum temperature at which  $\alpha$ -crystallin remains folded is essential for such assays. In this instance, the unfolding temperature was determined using CD (Fig. 6a). At 20° C our preparation of  $\alpha$ -crystallin is estimated to be only 4%  $\alpha$ -helical (Table 1), and shows only a minor increase during higher temperature incubations. A small increase in the CD signal at 193 nm was observed at temperatures up to 60° C; above this temperature, the CD signal at 200 nm changes from positive to negative, indicative of a loss in ordered structure. Deconvolution estimates

suggest an increase in unordered conformation above 60° C, at the expense of  $\beta$ -sheet and turn conformations. The tertiary/quaternary structure of  $\alpha$ -crystallin has been extensively characterised over a similar temperature range and has been shown to rapidly and irreversibly double in assembly size between 60 and 69° C [11], corresponding to the 'activated' form, whilst precipitating once above 70° C [48]. Considered in conjunction with the CD data, this suggests that increases in ordered  $\alpha$ -crystallin secondary structure may correlate with assembly into the higher molecular weight activated complex. The rapid increase in unordered secondary structure above 60° C is indicative of the aggregating state, and is unlikely to relate to its chaperone mechanism.  $\alpha$ -crystallin appears stable below this temperature; after a 16 hour incubation at 60° C, the CD spectrum is unaltered except for an increased 193 nm signal, described above, and scattering from the solution did not increase during incubation (Fig. 6b). The increase in CD signal at 193 nm is irreversible upon cooling to 20° C, and is indicative of structural changes associated with the previously proposed concept of a chaperone activation mechanism [11,49].

#### *Activity of $\alpha$ -crystallin*

$\alpha$ -crystallin was shown to be functional by its ability to suppress light scattering from a 1:1.17 M (based on monomer size) solution of  $\alpha$ -crystallin and  $\beta$ B2 at 60° C and above (Fig. 7a). At 60° C, un-chaperoned human  $\beta$ B2 begins to scatter light after ~450 seconds and reaches a plateau at ~3300 seconds. When incubated with  $\alpha$ -crystallin, light scattering remains constant and low over a one-hour period (Fig. 7b).

#### *Conformation of $\beta$ B2-crystallins bound to $\alpha$ -crystallin*

The conformation of  $\beta$ B2-crystallin bound to  $\alpha$ -crystallin was investigated using CD spectroscopy. Incubation was extended to 16 hours to promote increased  $\beta$ B2-crystallin association with  $\alpha$ -crystallin without exceeding 60° C, and was found to promote appreciable binding of both human and calf  $\beta$ B2 to  $\alpha$ -crystallin. Solutions were cooled and centrifuged, and CD spectra recorded to examine the complex under conditions that favour refolding. Spectra of solutions of  $\beta$ B2 and  $\alpha$ -crystallin ( $\beta$ B2- $\alpha$ ) prior to heating are identical to composite spectra of  $\alpha$ -crystallin and  $\beta$ B2-crystallin alone; there is no spectral indication of secondary structure change due to interaction. Light scattering did not increase during heat incubation, confirming that the chaperone complex of chaperone bound to substrate protein remained soluble. Spectra of chaperoned human and calf  $\beta$ B2-crystallins were obtained by subtracting the post-incubation spectrum of  $\alpha$ -crystallin from the post-incubation spectra of human and calf  $\beta$ B2- $\alpha$  solutions (Fig. 8), and compared to the spectra of un-chaperoned  $\beta$ B2-crystallins after equivalent incubations. Unchaperoned human  $\beta$ B2 and calf  $\beta$ B2 are not stable during this incubation; spectra of both appear only partially folded and of lower concentration following incubation. Chaperoned human and calf  $\beta$ B2 are retained in solution to a higher concentration but their CD spectra resemble those of partially refolded human  $\beta$ B2-crystallin, rather than the more structured CD spectra of aggregate material shown in Fig. 5.

The failure of chaperoned calf  $\beta$ B2 to refold under conditions that have been shown to favour full refolding following shorter incubation lends support to the idea that the aggregation prone pathway involves a non-native low-energy intermediate state, which is recognised and bound by  $\alpha$ -crystallin prior to aggregation. Binding of  $\alpha$ -crystallin to states that are aggregation-prone, but not yet precipitating, has also been described for  $\alpha$ -lactalbumin, in which the chaperone engages in kinetic competition with the aggregation pathway [50].

### **Discussion**

#### *A model for $\beta$ B2-crystallin unfolding and chaperone association*

By performing structural studies of both substrate protein ( $\beta$ B2) and  $\alpha$ -crystallin, it is possible to unite models for  $\beta$ B2-crystallin unfolding [36,44] and  $\alpha$ -crystallin chaperone activity [11,37,49]. Our observations lead us to conclude that calf and human  $\beta$ B2 share broadly similar unfolding pathways, but the overall reversibility of calf  $\beta$ B2 unfolding is due to sparse population of the partially unfolded intermediate state. It is interesting that these experiments do not conform with the assumption that destabilisation enhances aggregation. If it is assumed that the additional stability of human  $\beta$ B2 derives from its C-terminal domain, then the stability difference between the N and C domains becomes more marked. Thus, under conditions when the N-terminal domain unfolds, human  $\beta$ B2 is more likely to have a folded C-terminal domain with an interaction interface exposed that can act as an aggregation prone intermediate.

Our studies of the secondary structure of  $\alpha$ -crystallin show changes occurring at temperatures similar to those associated with tertiary/quaternary structure changes, in which increases in molecular weight are reported at 60 and 66°C [11,48]. This leads us to conclude that upon thermal activation,  $\alpha$ -crystallin undergoes an irreversible increase in ordered secondary structure, associated with assembly into the reported high molecular weight (80-mer) form. It is this form that associates with partially folded  $\beta$ B2 intermediates prior to aggregation in our experiments (Fig. 9). This finding is in agreement with a model in which population of a folding intermediate, rather than absolute energetic thresholds, can promote chaperone association [37]. In the case of human and calf  $\beta$ B2-crystallins, the intermediate states recognised by  $\alpha$ -crystallin are unable to correctly refold and, if not bound by  $\alpha$ -crystallin, will form insoluble aggregates. This mechanism has consequences for in vivo cataract formation: substrate protein sequestered by  $\alpha$ -crystallin must remain associated to avoid aggregation. This reduces the binding capacity of the  $\alpha$ -crystallin present in the lens, thus eventually overwhelming the chaperone system.

### **Acknowledgements**

The authors thank Drs. Orval Bateman and Myron Smith (Birkbeck College) for generously supplying protein samples and making available unpublished crystal structures. This work was supported by

BBSRC grants to BAW. CS acknowledges the financial support of the MRC. PE was supported by a BBSRC studentship

Stage 2(a) POST-PRINT

### References

1. Tardieu, A. (1998)  $\alpha$ -Crystallin quaternary structure and interactive properties control eye lens transparency. *Int. J. Biol. Macromol.* **22**, 211–217.
2. Trokel, S. (1962) The physical basis for transparency of the crystalline lens. *Invest. Ophthalmol.* **1**, 493–501.
3. Harding, J.J. and Crabbe, M.J.C. (1984) The lens: development, proteins, metabolism and cataract. The eye. 3rd edition. Academic Press, New York. 207–492.
4. Horwitz, J. (1992)  $\alpha$ -Crystallin can function as a molecular chaperone. *Proc. Natl. Acad. Sci. USA* **89**, 10449-10453.
5. Bloemendal, H., de Jong, W., Jaenicke, R., Lubsen, N.H., Slingsby, C., and Tardieu A. (2004) Ageing and vision: structure, stability and function of lens crystallins. *Prog. Biophys. Mol. Biol.* **86**, 407-485.
6. Brakenhoff, R.H., Aarts, H.J., Reek, F.H., Lubsen, N.H., and Schoenmakers, J.G. (1990) Human  $\gamma$ -crystallin genes. A gene family on its way to extinction. *J. Mol. Biol.* **216**, 519-532.
7. Lampi, K.J., Ma, Z., Shih, M., Shearer, T.R., Smith, J.B., Smith, D.L., and David, L.L. (1997) Sequence analysis of  $\beta$ A3,  $\beta$ B3, and  $\beta$ A4 crystallins completes the identification of the major proteins in young human lens. *J. Biol. Chem.* **272**, 2268-2275.
8. Robinson, N.E., Lampi, K.J., Speir, J.P., Kruppa, G., Easterling, M., and Robinson, A.B. (2006) Quantitative measurement of young human eye lens crystallins by direct injection Fourier transform ion cyclotron resonance mass spectrometry. *Mol. Vis.* **12**, 704-711.
9. Wilmarth, P.A., Tanner, S., Dasari, S., Nagalla, S.R., Riviere, M. A, Bafna, V., Pevzner, P.A., and David, L.L. (2006) Age-related changes in human crystallins determined from comparative analysis of post-translational modifications in young and aged lens: does deamidation contribute to crystallin insolubility? *J. Proteome Res.* **5**, 2554-2566.
10. Tardieu, A., Laporte, D., Licinio, P., Krop, B., and Delaye, M. (1986) Calf lens  $\alpha$ -crystallin quaternary structure. A three-layer tetrahedral model. *J. Mol. Biol.* **192**, 711-724.
11. Putilina, T., Skouri-Panet, F., Prat, K., Lubsen, N.H., and Tardieu, A. (2003) Subunit exchange demonstrates a differential chaperone activity of calf  $\alpha$ -crystallin toward  $\beta_{\text{LOW}}$ - and individual  $\gamma$ -crystallins. *J. Biol. Chem.* **278**, 13747-13756.
12. Aquilina, J.A., Benesch, J.L., Bateman, O.A., Slingsby, C., and Robinson, C.V. (2003) Polydispersity of a mammalian chaperone: mass spectrometry reveals the population of oligomers in  $\alpha$ B-crystallin. *Proc. Natl. Acad. Sci. USA* **100**, 10611-10616.
13. Kim, K.K., Kim, R., and Kim, S.H. (1998) Crystal structure of a small heat-shock protein. *Nature* **394**, 595-599.

14. van Montfort, R.L., Basha, E., Friedrich, K.L., Slingsby, C., and Vierling, E. (2001) Crystal structure and assembly of a eukaryotic small heat shock protein. *Nat. Struct. Biol.* **8**, 1025-1030.
15. Stampler, R., Kappe, G., Boelens, W., and Slingsby, C. (2005) Wrapping the  $\alpha$ -crystallin domain fold in a chaperone assembly. *J. Mol. Biol.* **353**, 68-79.
16. Sobott F., Benesch, J.L.P., Vierling, E., and Robinson, C.V. (2002) Subunit exchange of multimeric protein complexes. Real-time monitoring of subunit exchange between small heat shock proteins by using electrospray mass spectrometry. *J. Biol. Chem.* **277**, 38921-38929.
17. Basha, E., Friedrich, K.L., and Vierling, E. (2006) The N-terminal arm of small heat shock proteins is important for both chaperone activity and substrate specificity. *J. Biol. Chem.* **281**, 39943-39952.
18. Shashidharamurthy, R., Koteiche, H.A., Dong, J., and McHaourab, H.S. (2005) Mechanism of chaperone function in small heat shock proteins: dissociation of the HSP27 oligomer is required for recognition and binding of destabilized T4 lysozyme. *J. Biol. Chem.* **280**, 5281-5289.
19. Koteiche, H.A., and Mchaourab, H.S. (2006) Mechanism of a hereditary cataract phenotype. Mutations in alphaA-crystallin activate substrate binding. *J. Biol. Chem.* **281**, 14273-14279.
20. Bova, M.P., Ding, L.L., Horwitz, J., and Fung, B.K. (1997) Subunit exchange of  $\alpha$ A-crystallin. *J. Biol. Chem.* **272**, 29511-29517.
21. Das, K.P. and Surewicz, W.K. (1995) On the substrate specificity of alpha-crystallin as a molecular chaperone. *FEBS Lett.* **369**, 321-325.
22. Koteiche, H.A. and Mchaourab, H.S. (2003) Mechanism of chaperone function in small heat-shock proteins. Phosphorylation-induced activation of two-mode binding in alphaB-crystallin. *J. Biol. Chem.* **278**, 10361-10367.
23. Franzmann, T.M., Wuhr, M., Richter, K., Walter, S., and Buchner, J. (2005) The activation mechanism of Hsp26 does not require dissociation of the oligomer. *J. Mol. Biol.* **350**, 1083-1093.
24. Blundell, T.L., Lindley, P., Miller, L., Moss, D., Slingsby, C., Tickle, I., Turnell, B., and Wistow, G. The molecular structure and stability of the eye lens: X-ray analysis of  $\gamma$ -crystallin II. (1981) *Nature* **289**, 771-777.
25. Bax, B., Lapatto, R., Nalini, V., Driessen, H., Lindley, P. F., Mahadevan, D., Blundell, T. L., and Slingsby, C. (1990) X-ray analysis of  $\beta$ B2-crystallin and evolution of oligomeric lens proteins. *Nature* **347**, 776-780.
26. van Montfort, R.L., Bateman, O.A., Lubsen, N.H., and Slingsby, C. (2003) Crystal structure of truncated human  $\beta$ B1-crystallin. *Protein Sci.* **12**, 2606-2612.
27. Smith, M.A., Bateman, O.A., Jaenicke, R., and Slingsby, C. (2007) Mutation of interfaces in domain-swapped human betaB2-crystallin. *Protein Sci.* **16**, 615-625.

28. Bateman, O.A., Sarra, R., van Genesen, S.T., Kappe, G., Lubsen, N.H., and Slingsby, C. (2003) The stability of human acidic  $\beta$ -crystallin oligomers and hetero-oligomers. *Exp. Eye Res.* **77**, 409-422.
29. Kim, Y.H., Kapfer, D.M., Boekhorst, J., Lubsen, N.H., Bächinger, H.P., Shearer, T.R., David, L.L., Feix, J. B., and Lampi, K.J. (2002) Deamidation, but not truncation, decreases the urea stability of a lens structural protein,  $\beta$ B1-crystallin. *Biochemistry* **41**, 14076-14084.
30. Flaugh, S.L., Kosinski-Collins, M.S., and King, J. (2005) Contributions of hydrophobic domain interface interactions to the folding and stability of human  $\gamma$ D-crystallin. *Protein Sci.* **14**, 569-581.
31. Jaenicke, R. and Slingsby, C. (2001) Lens crystallins and their microbial homologs: structure, stability, and function. *Crit. Rev. Biochem. Mol. Biol.* **36**, 435-499.
32. Derham, B.K. and Harding, J.J. (1999)  $\alpha$ -crystallin as a molecular chaperone. *Prog. Retin. Eye Res.* **18**, 463-509.
33. Lampi, K.J., Kim, Y.H., Bächinger, H.P., Boswell, B.A., Lindner, R.A., Carver, J.A., Shearer, T.R., David, L.L., and Kapfer, D.M. (2002) Decreased heat stability and increased chaperone requirement of modified human  $\beta$ B1-crystallins. *Mol. Vis.* **8**, 359-366.
34. Kosinski-Collins, M.S., and King, J. (2003) In vitro unfolding, refolding, and polymerization of human  $\gamma$ D crystallin, a protein involved in cataract formation. *Protein Sci.* **12**, 480-490.
35. Flaugh, S.L., Kosinski-Collins, M.S., and King, J. (2005) Interdomain side-chain interactions in human  $\gamma$ D crystallin influencing folding and stability. *Protein Sci.* **14**, 2030-2043.
36. Wieligmann, K., Mayr, E.M., and Jaenicke, R. (1999) Folding and self-assembly of the domains of  $\beta$ B2-crystallin from rat eye lens. *J. Mol. Biol.* **286**, 989-994.
37. Sathish, H.A., Koteiche, H.A., and McHaourab, H.S. (2004) Binding of destabilized  $\beta$ B2-crystallin mutants to  $\alpha$ -crystallin: the role of a folding intermediate. *J. Biol. Chem.* **279**, 16425-16432.
38. Horwitz, J., McFall-Nagai, M., Ding, L.L., and Yaron, O. (1986) Duncan, G., (Ed.), *Topics in Aging Research in Europe*, 16. Eurage, Holland, pp. 227-240.
39. Slingsby, C., and Bateman, O.A. (1990) Rapid separation of bovine  $\beta$ -crystallin subunits  $\beta$ B1,  $\beta$ B2,  $\beta$ B3,  $\beta$ A3 and  $\beta$ A4. *Exp. Eye Res.* **51**, 21-26.
40. Miles, A.J., Wien, F., and Wallace, B.A. (2004) Redetermination of the extinction coefficient of camphor-10-sulfonic acid, a calibration standard for circular dichroism spectroscopy. *Anal. Biochem.* **335**, 338-339.
41. Provencher, S.W. and Glockner, J. (1981) Estimation of globular protein secondary structure from circular dichroism. *Biochemistry* **20**, 33-37.

42. Sreerama, N., Venyaminov, S.Y., and Woody, R.W. (2001) Analysis of protein circular dichroism spectra based on the tertiary structure classification. *Anal. Biochem.* **299**, 271-274.
43. Evans, P., Bateman, O.A., Slingsby, C., and Wallace, B.A. (2007) A reference dataset for circular dichroism spectroscopy tailored for the betagamma-crystallin lens proteins. *Exp. Eye. Res.* **84**, 1001-1008
44. Fu, L. and Liang, J.J. (2002) Unfolding of human lens recombinant betaB2- and gammaC-crystallins. *J. Struct. Biol.* **139**, 191-198.
45. MacDonald, J.T., Purkiss, A.G., Smith, M.A., Evans, P., Goodfellow, J.M., and Slingsby, C. (2005) Unfolding crystallins: the destabilizing role of a  $\beta$ -hairpin cysteine in  $\beta$ B2-crystallin by simulation and experiment. *Protein Sci.* **14**, 1282-1292.
46. Trinkl, S., Glockscher, R., and Jaenicke, R. (1994) Dimerization of  $\beta$ B2-crystallin: The role of the linker peptide and the N- and C-terminal extensions. *Protein Sci.* **3**, 1392-1400.
47. Wang, K., and Spector, A. (1994) The chaperone activity of bovine alpha crystallin. Interaction with other lens crystallins in native and denatured states. *J. Biol. Chem.* **269**, 13601-13608
48. Skouri-Panet, F., Quevillon-Cheruel, S., Michiel, M., Tardieu, A., and Finet, S. (2006) sHSPs under temperature and pressure: the opposite behaviour of lens alpha-crystallins and yeast HSP26. *Biochim Biophys Acta.* **1764**, 372-383.
49. Mchaourab, H.S., Dodson, E.K., and Koteiche, H.A. (2002) Mechanism of chaperone function in small heat shock proteins. Two-mode binding of the excited states of T4 lysozyme mutants by alphaA-crystallin. *J. Biol. Chem.* **277**, 40557-40566.
50. Lindner, R.A., Treweek, T.M., and Carver, J.A. (2001) The molecular chaperone alpha-crystallin is in kinetic competition with aggregation to stabilize a monomeric molten-globule form of alpha-lactalbumin. *Biochem. J.* **354**, 79-87.



## Figures

**Fig. 1.** Sequence differences in human and calf  $\beta$ B2-crystallin. a) Alignment of  $\beta$ B2-crystallin sequences. Sequences are divided into N- and C-terminal extensions, N- and C-terminal domains, and inter-domain linker, with  $\beta$ -strands annotated according to the human  $\beta$ B2-crystallin structure (1YQT). Residues are coloured grey where they differ from the human sequence. Rat sequence is shown for comparison, as previous  $\beta$ B2 unfolding models used rat protein. Uppercase 'N' and 'C' denote the N- and C-terminal domains. b) Structure of human  $\beta$ B2-crystallin, showing location of C-terminal domain sequence differences between human and calf orthologues. Residues 1-13 of the N-terminal extension and 194-204 of the C-terminal extension are not visible in the crystal structures.

**Fig. 2.** Aggregation of human and calf  $\beta$ B2-crystallins. a) Loss of  $\beta$ B2-crystallin from solution following incubation at 10 minutes at elevated temperatures, followed by cooling on ice for 5 minutes, then centrifugation for 5 minutes to remove large aggregates. The absorbance at 280 nm represents the amount of protein retained in solution following thermal challenge. b) Fluorescence light scattering from human and calf  $\beta$ B2-crystallin samples at elevated temperatures.

**Fig. 3.** Thermal and chemical unfolding of  $\beta$ B2-crystallins. a) Thermal unfolding of human and calf  $\beta$ B2-crystallins, monitored by circular dichroism at 195 nm. Samples were incubated for 10 minutes at the given temperature. b) Urea-induced unfolding of human and calf  $\beta$ B2-crystallins, monitored by circular dichroism at 222 nm.

**Fig. 4.** Unfolding and refolding of human and calf  $\beta$ B2-crystallins monitored by circular dichroism spectroscopy. a) Thermal unfolding of calf  $\beta$ B2-crystallin. b) Refolding of calf  $\beta$ B2-crystallin at 20° C. c) Thermal unfolding of human  $\beta$ B2-crystallin. d) Refolding of human  $\beta$ B2-crystallin at 20° C.

**Fig. 5.** Secondary structure of soluble and aggregated human  $\beta$ B2-crystallins. Circular dichroism spectra were collected of pre- and post-centrifugation human  $\beta$ B2-crystallin samples following partial thermal refolding of human  $\beta$ B2-crystallin. The sample was incubated for 10 minutes at 90° C, before refolding for 15 minutes at 20° C. Spectra were collected at 20° C, then the sample was centrifuged for 5 minutes to remove aggregate, and spectra collected of the aggregate-free sample. The difference spectrum is assumed to represent the contribution of the protein aggregate to the initial cooled spectrum. Spectra are scaled to  $\Delta\epsilon$  in accordance with the starting concentration, but post-heating samples will be lower in concentration.

**Fig. 6.** Thermal stability of  $\alpha$ -crystallin. a) Thermal unfolding of calf  $\alpha$ -crystallin monitored by circular dichroism. Fresh samples were used for each temperature increment, and incubated for 10 minutes prior to data collection. b) Long-term thermal stability of bovine lens  $\alpha$ -crystallin measured by circular dichroism spectroscopy. The sample was heated to 20° C, equilibrated for 10 minutes, and circular dichroism spectra collected. The sample temperature was then raised to 60° C, equilibrated for a further 10 minutes, and the circular dichroism spectra recorded. After 16 hours at 60° C the sample temperature was reduced to 20° C, equilibrated for 10 minutes, and the CD spectra collected. Throughout the experiment the voltage applied to the photomultiplier detector remained constant, indicative of no alteration in absorbance or scattering during incubation.

**Fig. 7.** Suppression of light scattering from  $\beta$ B2-crystallin by  $\alpha$ -crystallin measured using fluorescence. a) Temperature dependence of light scattering by  $\beta$ B2-crystallin in presence and absence of  $\alpha$ -crystallin. b) Time-dependence of light scattering from human  $\beta$ B2-crystallin at 60° C, in the presence and absence of  $\alpha$ -crystallin. In this case the instrument excitation and emission slits reduced to 5 nm to avoid exceeding the instrument response range as the scattering increased.

**Fig. 8.** Unfolding of chaperone-associated  $\beta$ B2-crystallin. Comparison of circular dichroism spectra of un-chaperoned  $\beta$ B2-crystallin with those of chaperoned  $\beta$ B2-crystallin following incubation at 60° C for 16 hours. Chaperoned  $\beta$ B2-crystallin spectra were calculated from post-incubation spectra solutions of  $\beta$ B2-crystallin in complex with  $\alpha$ -crystallin, minus the post-incubation spectra of  $\alpha$ -crystallin alone. To obtain optimal data, spectra were recorded in cells of various pathlength: all data has been normalised to  $\theta$  (mdegs) in a 0.05 cm pathlength.

**Fig. 9.** Schematic model of the unfolding, aggregation and  $\alpha$ -crystallin association of  $\beta$ B2-crystallin under thermal challenge.  $\beta$ B2-crystallin: unfolding according to a three state model, with a monomeric partially-unfolded intermediate, and an aggregation pathway that competes with productive refolding. D=dimer, I=partially-folded intermediate, I\*=pre-aggregation low-energy state, U=unfolded. Arrows shown in broken blue line represent transitions that have been proposed but not observed experimentally. If these transitions are reversible, kinetics of the 2I→I\* step may facilitate kinetic partitioning between productive and aggregation-prone pathways.  $\alpha$ -crystallin: Tertiary model based on literature observations of approximate doubling in size of the  $\alpha$ -crystallin complex above 60° C, and aggregation at temperatures above 70° C [11;48]. Undetermined oligomeric size and aggregation tendencies of  $\alpha$ -crystallin above 70° C denoted on figure by '?' and '+' respectively. The complex of  $\alpha$ -crystallin with bound  $\beta$ B2-

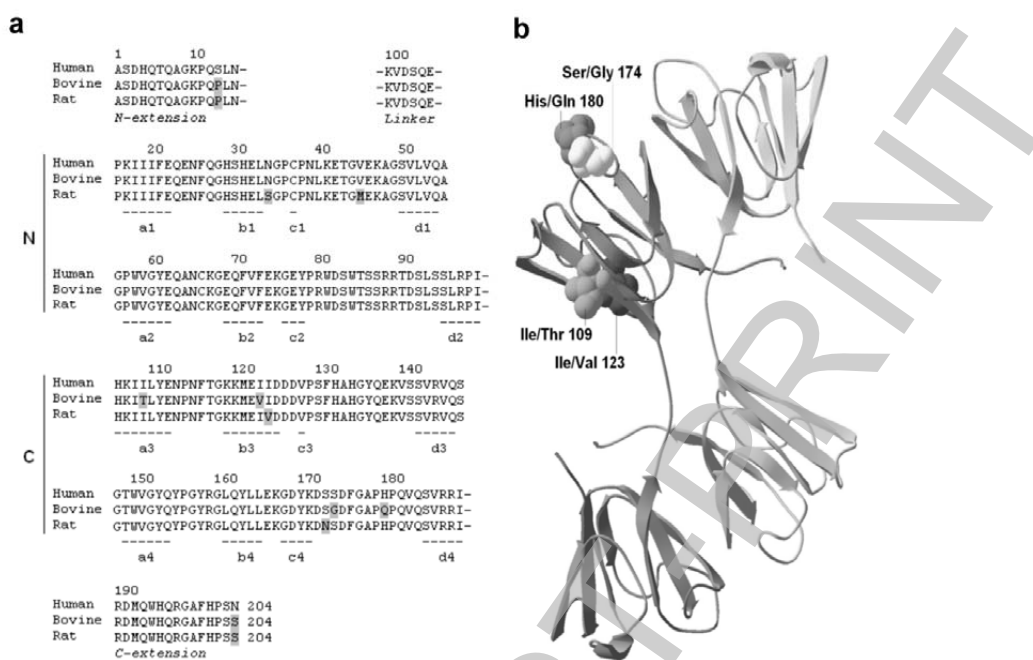
crystallin,  $\alpha$ -I\*, is portrayed as the activated oligomeric state of  $\alpha$ -crystallin with I\* particles adhering to the assembly.

Stage 2(a) POST-PRINT

Table 1. Secondary structure of  $\alpha$ -crystallin, showing changes in response to elevated temperature. NRMSD denotes root mean squared deviations in fit between experimental and reconstructed circular dichroism data.

Temp. (°C)	Estimated Secondary Structure Fraction				NRMSD
	$\alpha$	$\beta$	Turn	Other	
10	0.05	0.36	0.20	0.40	0.06
20	0.04	0.36	0.20	0.40	0.05
30	0.05	0.37	0.20	0.39	0.05
40	0.05	0.37	0.20	0.39	0.05
50	0.05	0.37	0.20	0.37	0.04
60	0.07	0.36	0.21	0.36	0.03
70	0.08	0.32	0.18	0.42	0.03
80	0.08	0.29	0.16	0.47	0.03
90	0.08	0.27	0.15	0.50	0.04

**Figure 1**



THIS IS NOT THE FINAL VERSION - see doi:10.1042/BJ20070993

Figure 2

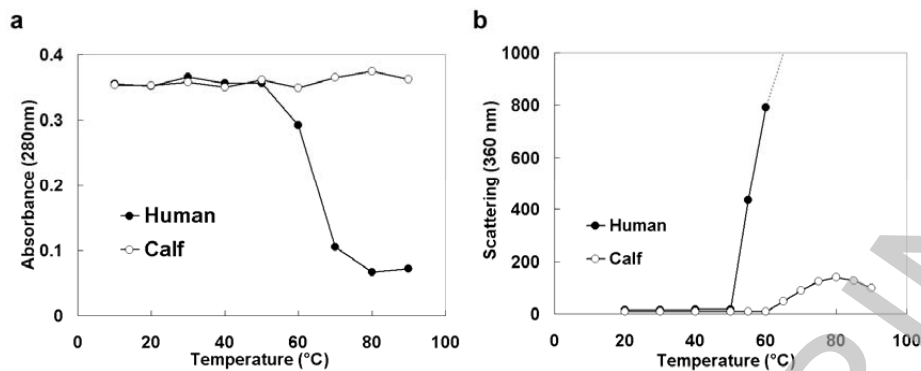


Figure 3

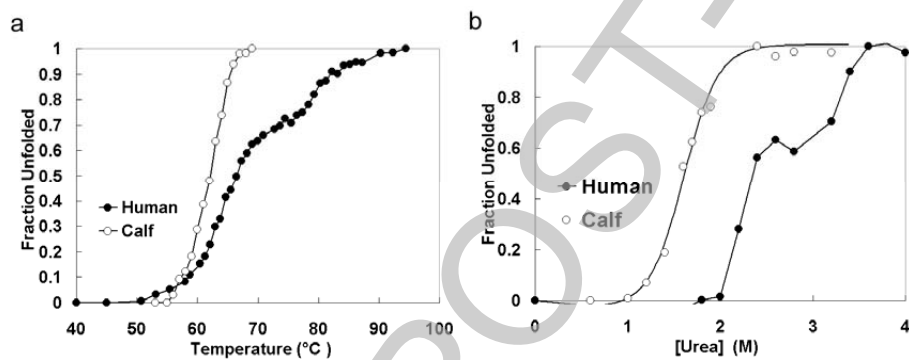


Figure 4

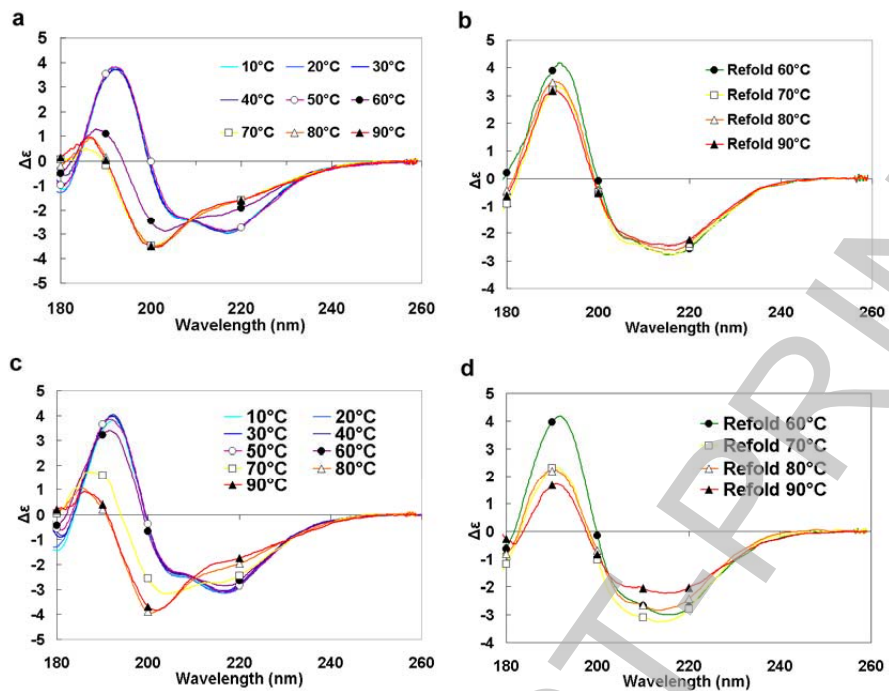


Figure 5

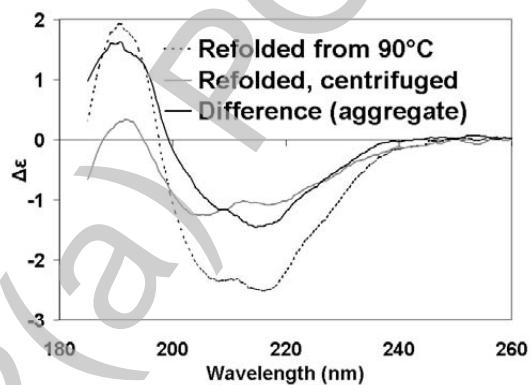


Figure 6

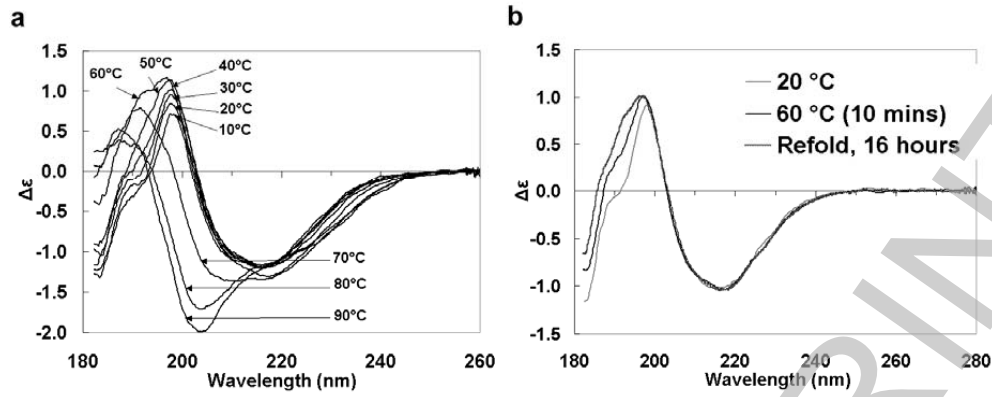


Figure 7

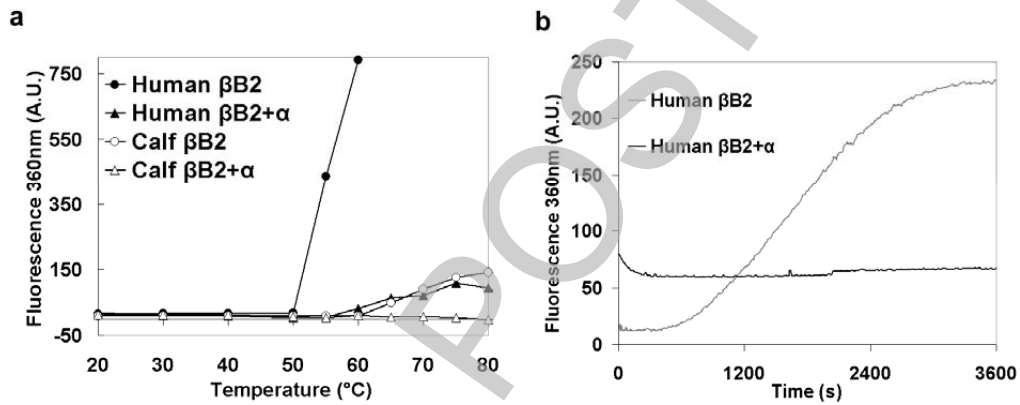




Figure 8

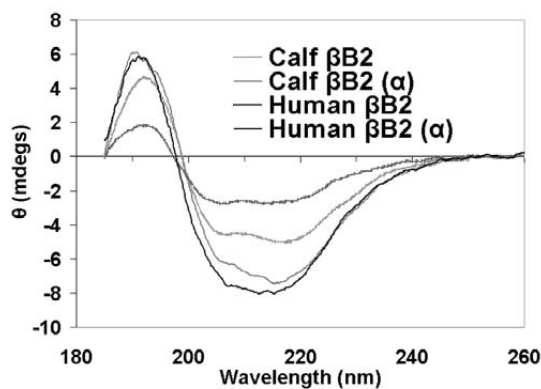


Figure 9

